

A Novel Ultrasound-Vibration Composite Sensor for Defects Detection of Electrical Equipment

Original

A Novel Ultrasound-Vibration Composite Sensor for Defects Detection of Electrical Equipment / Zhang, Z.; Li, J.; Song, Y.; Sun, Y.; Zhang, X.; Hu, Y.; Guo, R.; Han, X.. - In: IEEE TRANSACTIONS ON POWER DELIVERY. - ISSN 0885-8977. - ELETTRONICO. - 37:5(2022), pp. 4477-4480. [10.1109/TPWRD.2022.3171713]

Availability:

This version is available at: 11583/2994651 since: 2024-11-21T10:16:05Z

Publisher:

Institute of Electrical and Electronics Engineers

Published

DOI:10.1109/TPWRD.2022.3171713

Terms of use:

This article is made available under terms and conditions as specified in the corresponding bibliographic description in the repository

Publisher copyright

IEEE postprint/Author's Accepted Manuscript

©2022 IEEE. Personal use of this material is permitted. Permission from IEEE must be obtained for all other uses, in any current or future media, including reprinting/republishing this material for advertising or promotional purposes, creating new collecting works, for resale or lists, or reuse of any copyrighted component of this work in other works.

(Article begins on next page)

A Novel Ultrasound-Vibration Composite Sensor for Defects Detection of Electrical Equipment

Zhaoyu Zhang, Junhao Li, Yanfeng Song, Yuan Sun, Xuanrui Zhang, Yidan Hu, Ruochen Guo and Xutao Han

Abstract—The faults of electrical equipment are mainly generated by electrical and mechanical defects, which are usually detected by external ultrasonic and vibration sensors respectively. To improve the accuracy and efficiency of the diagnosis, a novel ultrasound-vibration composite sensor (UVCS) which can detect ultrasound and vibration acceleration signals synchronously at the same place, is proposed and developed scientifically in this paper. The working principle of UVCS is based on the combination of the mass and the backing as well as the steel base and matching layer, and the structure is improved reasonably. Furthermore, the ultrasound and vibration signals can be separated by filtering. In addition, the test results on a 110kV GIS show the high precision and reliability of UVCS and illustrate the superiority in practical application.

Index Terms—Electrical equipment, electrical and mechanical defects detection, ultrasonic sensor, vibration acceleration sensor

I. INTRODUCTION

THE large electrical equipment, such as power transformer, gas insulated switchgear (GIS), takes an fundamental position in power grid, and the operating state diagnosis is indispensable. Since this kind of equipment is not only important electrical equipment, but also complex mechanical equipment, its faults are generally caused from electrical and mechanical defects, such as partial discharge (PD) of insulation deterioration, poor contact of conductors in GIS and winding deformation in power transformer. Actually, the two defects are correlative. Mechanical vibration is one of the main reasons of electrical defect in some cases, while the severity of electrical defect can reflect the mechanical state [1]. Therefore, it is essential to obtain complementary information of the two defects to assess the state of electrical equipment reasonably.

It is recognized that ultrasound (frequency > 20 kHz) can be generated by partial discharge in electrical equipment, so the ultrasonic sensor, which is also called acoustic emission (AE) sensor in some technical literatures, is usually applied to detect electrical defect [2]. However, it is not effective to detect mechanical defect which is generally measured by vibration acceleration (frequency < 4 kHz) sensor [3]. In previous studies, ultrasonic and vibration signals are always detected and analyzed independently. The two types of sensors are usually installed on the shell of electrical equipment to detect the defect at different positions, or at the same position alternatively. The former hardly ensures the identity of detection location, and the latter cannot make the detection synchronous. Therefore, this independent detection is not precise for combined analysis nor efficient, and it is hard to study the relationship between mechanical and electrical defects of electrical equipment by the two signals.

In order to address this problem, this paper develops a novel sensor which is able to concurrently acquire accurate ultrasonic and vibration acceleration signals at the same position. The output composite signal can be separated by filters to vibration acceleration signal (1 Hz - 4 kHz) and ultrasonic signal (above 20 kHz). The joint detection is superior at less detection devices and cost, so that more composite sensors can be used in online detection. In addition, the multi-signal can be collected through one kit, simplifying the detection process and enriching the information, which makes it convenient to do comprehensive analysis for PD and mechanical defect. Finally, defect detection efficiency is improved [4]. Based on the proposed sensor, a test is carried out on a 110 kV GIS, comparing with two industrial sensors, the results verify the availability of this novel composite sensor.

II. THE PRINCIPLE AND STRUCTURE OF NOVEL UVCS

The UVCS developed in this paper is based on the principles of piezoelectric ultrasonic and vibration acceleration sensors. Both of them have the similar structure which are described in Fig. 1(a) and (b) [5,6].

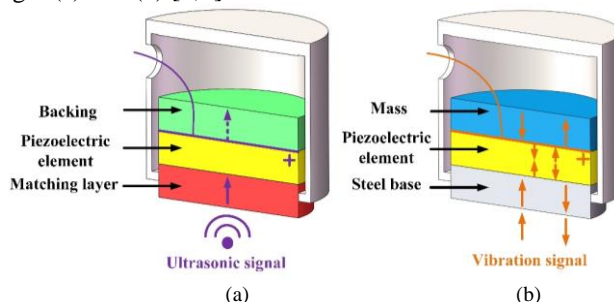


Fig. 1. Structures of piezoelectric ultrasonic and vibration acceleration sensor. (a) Ultrasonic sensor. (b) Vibration acceleration sensor

The fundamental principle of the composite sensor is using a mass backing as the backing of ultrasonic part and as the mass of vibration part at the same time, as shown in Fig. 2. In addition, the metal matching layer is used as the matching layer of ultrasonic part and as the steel base of vibration part at the same time. In the low frequency range (1 Hz ~ 4 kHz, vibration), because the mass backing is made of high density metal, it works as mass and can apply inertial force to the piezoelectric ceramics. The metal matching layer works as a steel base due to its good hardness and conductivity, which can better protect the internal components, transmit the vibration signal stably, and form the sealed ground potential with the housing to remove the external electromagnetic interference. In the high frequency range (above 20 kHz, ultrasound, more penetrative), the mass backing acts as backing which can well absorb backward ultrasonic wave to reduce the interference of reflection and improve the resolution and frequency response

range through the tungsten powder inside [7]. At this time, the metal matching layer can improve the transmission efficiency of ultrasonic signal by matching the acoustic impedance of the measured object and the piezoelectric ceramic.

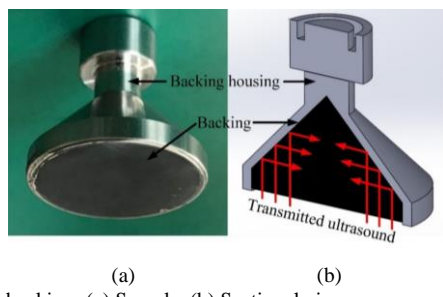


Fig. 2. Mass backing. (a) Sample. (b) Sectional view.

For GIS, the acoustic impedance of GIS enclosure and PZT-5 are 14.3 MRayl and 32.7 MRayl, so that of the matching layer should be 21.6 MRayl to acquire the highest energy transmission according to acoustic matching formula [8]. However, the matching layer of ultrasound sensor is generally made of ceramic (above 30 MRayl) or steel (above 40 MRayl). In this paper, the matching layer of the UVCS is made of 6061 aluminum alloy (19.6 MRayl) due to its appropriate acoustic impedance and good hardness and conductivity.

The large mass stainless steel (7.95 g/cm^3) tapered housing of the mass backing is designed in this paper, the backing inside is made by mixing tungsten powder and epoxy resin in 1:4 proportion [7]. Enough mass and large acoustic attenuation performance of the mass backing allow it to serve as both the mass and the backing [5]. In addition, the design of the tapered housing can well counteract the backward ultrasound interference and improve the signal-to-noise ratio (SNR).

The two piezoelectric ceramics (PZT-5) are pasted by conductive glue to enhance sensitivity, the diameters and thicknesses are 20 mm and 4 mm respectively. The thickness of matching layer is 6 mm according to quarter wavelength theory, and the surface of it is evenly brushed by thin epoxy paint (insulation) to remove the interference from the object.

Based on the above, the UVCS designed in this paper consists of mass backing, piezoelectric ceramic, acoustic matching layer, lead wire, and shell. Because the characteristic bands of mechanical defect and PD in GIS concentrate on 1 Hz ~ 4 kHz and 20 kHz ~ 100 kHz, the resonant frequency and detection band of UVCS are designed to 45 kHz and 1 Hz ~ 100 kHz respectively. The work temperature range is $-40 \text{ }^\circ\text{C} \sim 200 \text{ }^\circ\text{C}$. The dimension and weight are 26 mm OD \times 40 mm H and 101 g. The structure and the sample of UVCS are depicted in Fig. 3(a) and (b).

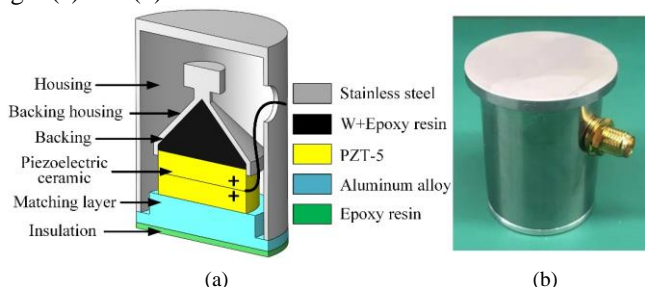


Fig. 3. Structure and sample of UVCS. (a) Structure. (b) Sample.

The UVCS has been calibrated for the sensitivity of vibration

and ultrasound according to ISO 16063-21-2003 and ASTM E1106-2002, the results are shown in Fig. 4. The mean sensitivity is 74 dB (ref 1 V/(m/s)) for ultrasound and is 400 mV/g for vibration after amplification.

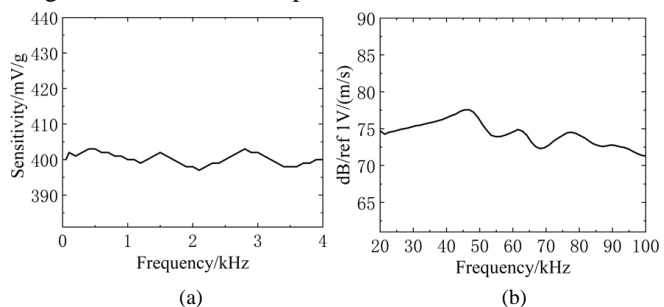


Fig. 4. Calibration of UVCS. (a) Vibration sensitivity. (b) Ultrasonic sensitivity.

III. PD AND VIBRATION MEASUREMENT OF GIS

To test the performance of UVCS, the test is carried out on a 110kV GIS which is filled with 0.45 MPa SF₆ gas. The experimental system is shown in Fig. 5. The disconnecter is located in the middle gas chamber of GIS on which the UVCS and two industrial ultrasonic and vibration sensors are installed. The information of two industrial sensors is shown in Table 1. The three signals of the sensors and the voltage of divider are recorded through the TEK4054 oscilloscope with 1.25 MS/s sampling rate.

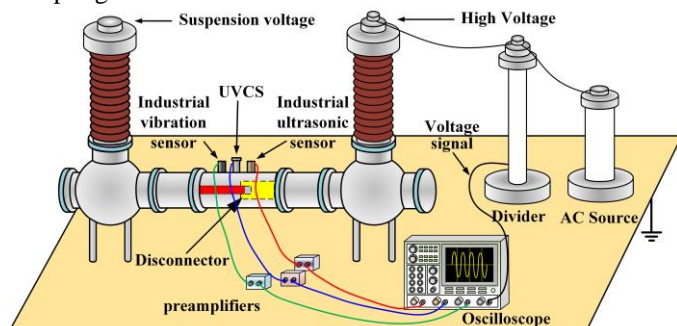


Fig. 5. The experimental system

TABLE 1
THE INFORMATION OF INDUSTRIAL ULTRASONIC AND VIBRATION SENSORS

Main parameters	Industrial Ultrasonic Sensor	Industrial Vibration Sensor
Working Frequency Range	20 kHz ~ 140 kHz	1 Hz ~ 4 kHz
Mean Sensitivity	80 dB (ref 1 V/(m/s))	300 mV/g
Resonant frequency	40 kHz	16 kHz

The excitation voltage is 160 kV, and the disconnecter inside the GIS is set to good contact (contact resistance: 112 $\mu\Omega$) and poor contact (contact resistance: 455 $\mu\Omega$). This typical poor contact defect is able to generate both PD and abnormal mechanical vibration under high electric field.

The signals of the three sensors on GIS enclosure under normal and critical states are depicted in Fig. 6 and Fig. 7. Each one consists of 6 figures. The original signal is easily interfered due to the high frequency noise from complicated electromagnetic environment, therefore, it is necessary to separate and amplify the output signal of the UVCS. The original signal of the UVCS is firstly filtered by low pass filter

(cutoff frequency: 120 kHz) for reducing noise and the result is shown in the second figure. And then the result is filtered by low and high pass filters (cutoff frequencies: 4 kHz and 20 kHz) to acquire the PD and vibration signals, which are shown in third and fifth figures respectively. The signals of industrial ultrasonic sensor (IUS) and industrial vibration acceleration sensors (IVS) are shown in fourth and sixth figures.

Fig. 6 compares the PD (above 20 kHz) and vibration (under 4 kHz) signals of the three sensors when disconnector stays good contact. On one hand, neither of the UVCS and industrial ultrasonic sensor detects PD impulses. On the other hand, the UVCS and industrial vibration sensor detect the same vibration signals which mainly contain 100 Hz vibration and a little other harmonics, because the electric field force is in direct proportion to double power frequency (100 Hz) and the contact state of the whole GIS is not absolutely ideal [9]. The results indicate that under good contact, there is no PD in GIS and the vibration is almost only characterized by 100 Hz.

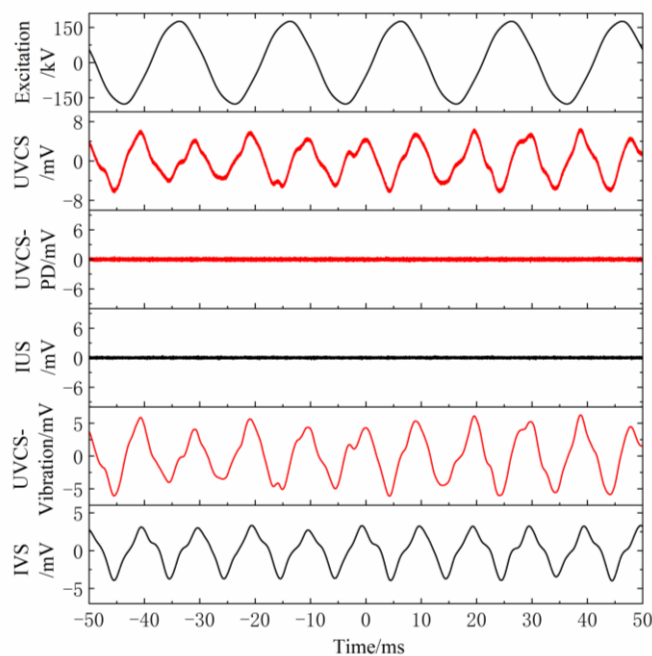


Fig. 6. The signals of three sensors on GIS shell under good contact

Fig. 7 compares the PD and vibration signals of the three sensors when disconnector stays poor contact. The signal of UVCS is superposition of PD and vibration signals. The UVCS-PD and industrial ultrasonic sensor are identical in time and magnitude. The pulses appear when the excitation voltage reaches about ± 130 kV in a period, which are a little prior to the peak (160 kV). This is because the disconnector has a poor contact, the air gap between high voltage contact and suspension contact is too little to withstand the large electric potential difference, which results in regular discharges finally. Therefore, it is recognized as typical floating discharge. Besides, the vibration signals of the UVCS and industrial vibration sensor still have main 100 Hz proportion, while there are more apparent high frequencies harmonics on GIS under poor contact. The abnormal vibration is generated because the poor contact of disconnector makes the contact resistance larger and the GIS mechanical state changes [9]. Moreover, these harmonics detected by UVCS are larger than that of industrial

vibration sensor, which means the UVCS is more sensitive in vibration detection.

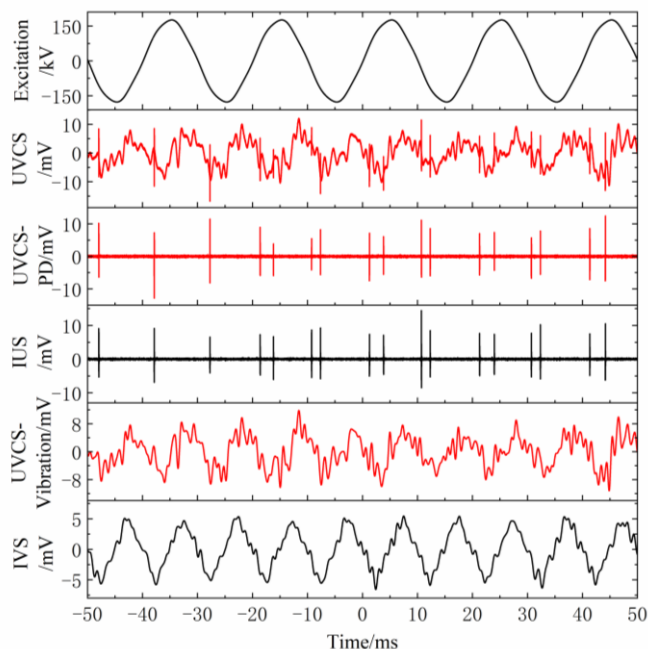


Fig. 7. The signals of three sensors on GIS shell under poor contact

Comparing Fig. 6 and Fig. 7, it can be found that the UVCS is able to detect the same PD pulses and vibration signals on GIS enclosure as the two industrial sensors.

IV. CONCLUSION

This paper proposes a novel ultrasound-vibration composite sensor to diagnose the electrical and mechanical defects of electrical equipment. The performance of UVCS is tested by comparing with industrial ultrasonic and vibration sensors on a 110 kV GIS PD and mechanical vibration experiment platform. The results evidently show that the UVCS can precisely detect both the vibration and ultrasonic signals simultaneously at the same position with high sensitivity. The signals can reflect PD and mechanical defect. It provides a more efficient, comprehensive and convenient detection method for defects diagnosis of electrical equipment.

REFERENCES

- [1] B. Liu, H. Ma and P. Ju, "Partial discharge diagnosis by simultaneous observation of discharge pulses and vibration signal," in *IEEE Transactions on Dielectrics and Electrical Insulation*, vol. 24, no. 1, pp. 288-295, Feb. 2017, doi: 10.1109/TDEI.2016.006072.
- [2] D. Antony and G. S. Punekar, "Noniterative Method for Combined Acoustic-Electrical Partial Discharge Source Localization," in *IEEE Transactions on Power Delivery*, vol. 33, no. 4, pp. 1679-1688, Aug. 2018, doi: 10.1109/TPWRD.2017.2769159.
- [3] M. Iorgulescu, R. Beloiu and M. O. Popescu, "Vibration monitoring for diagnosis of electrical equipment's faults," 2010 12th International Conference on Optimization of Electrical and Electronic Equipment, 2010, pp. 493-499, doi: 10.1109/OPTIM.2010.5510332.
- [4] J. Li, X. Han, Z. Liu and X. Yao, "A Novel GIS Partial Discharge Detection Sensor With Integrated Optical and UHF Methods," in *IEEE Transactions on Power Delivery*, vol. 33, no. 4, pp. 2047-2049, Aug. 2018, doi: 10.1109/TPWRD.2016.2635382.
- [5] Z. Feng and Z. Yufeng, "Research Progress of Mechanical Vibration Sensors," 2020 3rd World Conference on Mechanical Engineering and

Intelligent Manufacturing (WCMEIM), 2020, pp. 412-416, doi: 10.1109/WCMEIM52463.2020.00093.

- [6] H. D. Ilkhechi and M. H. Samimi, "Applications of the Acoustic Method in Partial Discharge Measurement: A Review," in *IEEE Transactions on Dielectrics and Electrical Insulation*, vol. 28, no. 1, pp. 42-51, February 2021, doi: 10.1109/TDEI.2020.008985.
- [7] Zhang, W. , et al. "Backing layers on electroacoustic properties of the acoustic emission sensors." *Applied Acoustics* 156.DEC.(2019):387-393.
- [8] Rathod, Vivek T. "A Review of Acoustic Impedance Matching Techniques for Piezoelectric Sensors and Transducers." *Sensors* 20.14(2020):4051.
- [9] Y. Yang, M. Suliang, W. Jianwen, J. Bowen, L. Weixin and L. Xiaowu, "Fault Diagnosis in Gas Insulated Switchgear Based on Genetic Algorithm and Density- Based Spatial Clustering of Applications With Noise," in *IEEE Sensors Journal*, vol. 21, no. 2, pp. 965-973, 15 Jan.15, 2021, doi: 10.1109/JSEN.2019.2942618.